Cosmic Radiation Intensity-Time Variations and Their Origin. I. Neutron Intensity Variation Method and Meteorological Factors*

J. A. SIMPSON, W. FONGER, AND S. B. TREIMAN†
Institute for Nuclear Studies, University of Chicago, Chicago, Illinois
(Received December 29, 1952)

An experimental method has been developed for extending the study of primary cosmic radiation intensity variations *vs* time to the low energy portion of the primary particle spectrum by measuring the nucleonic component intensity within the atmosphere. It is pointed out that this extension of intensity variation observations to the low energies now makes it possible to determine the energy dependence of primary intensity variations as well as to determine the intensity variations with time. The possibility of determining acceleration, perturbation, or injection processes within the solar system as the origin of intensity-time variations is considered. A phenomenological outline of kinds of intensity variations with definitions is presented and their relation to the present studies are discussed. The detector system is a pile structure of lead and paraffin within which the rate of local neutron production is measured by $B^{10}F_3$ proportional counters. Details on the large geomagnetic latitude effect of the nucleonic component or local neutron production are discussed.

The quantitative problem of relating intensity-time variations outside the atmosphere to pile neutron production deep in the atmosphere has been treated for primary energies below ~15 Bev for protons and ~7 Bev per nucleon for nuclei of $Z>1$. In particular, the contributions of primary protons and alpha-particles to the neutron yield in a pile are considered. The general problem of variations (a) due to primary intensity changes, (b) due to geomagnetic field variations, and (c) due to changing meteorological conditions are considered for nucleonic component measurements. The atmospheric pressure coefficient α is essentially constant over the geomagnetic latitude range $\lambda=0°$ to $\lambda>54°$N and for atmospheric depths >600 g-cm^{-2} (mountain altitudes or lower). $\alpha=-(0.94\pm0.03)$ percent/mm Hg. The difficulties in determining α due to accidental correlations with primary intensity variations is discussed, and a modified method for computing α is illustrated. The effect of atmospheric temperature variations upon observed pile neutron intensity is evaluated by a study of the upper limit contributions which π and μ mesons make as links in the nucleonic cascade. The evidence, including a two month temperature-cosmic-ray intensity correlation study, indicates a negligibly small local or atmospheric temperature coefficient for the nucleonic component.

Pile designs are given both for a simple pile standard which may be constructed anywhere for inter-calibration of experiments and for a 12 counter pile which produces ~7000 counts per minute at $\lambda=48°$ and altitude 680 g-cm^{-2}. Details are presented on the associated instrumentation. At the present time continuously operating piles are located at geomagnetic latitudes $\lambda=0°$, 29°N, 42°N, 48°N, and 52°N in the geographic longitude interval 75°–106°W.

I. INTRODUCTION

ALTHOUGH variations of cosmic radiation intensity with time have been studied extensively for over 35 years using charged particle detectors,[1,2] many of the reported variations are not well established, and in most cases their origins are not understood. In view of this we wish to investigate the possibility for further progress in resolving these difficulties. The magnitudes of the reported intensity-time variations are small and difficult to isolate from variations and fluctuations not related to the primary radiation. Since all continuous recorders of radiation intensity are restricted to mountain altitudes or lower, more than ~80 percent of the detected charged particles are produced by primaries having higher momenta than the equatorial latitude cut-off value ($\gtrsim$15 Bev/c for protons) for the terrestrial magnetic field. Hence, aside from the relatively rare and large solar flare effects[3] the continuous observation of intensity variations by charged particle detectors is limited to the high energy portion of cosmic radiation spectrum.

In order to extend measurements of intensity variations to primary particles of significantly lower energy, we require, for continuous observations, that the secondary radiation from these low energy primary particles be observed at large atmospheric depths. Recently the neutrons and low energy nuclear disintegrations from the nucleonic component were found to possess a larger geomagnetic latitude effect than any other secondary component,[4] and measurements using this component have indicated the feasibility of extending observations of temporal variations to the *low* energy portion of the primary particle spectrum.[4–7] Consequently we have been reinvestigating the origin of intensity-time variations, and in this paper we discuss some of the physical and experimental aspects of the problem.

Primary intensity variations have their origins exclusively in accelerating (decelerating) processes or perturbations involving a portion of the observed primary particle radiation distribution. Since acceleration theories generally lead to the prediction of particle energy spectrums, it is particularly important to extend measurements to the low energy spectrum to

* Assisted by the Office of Scientific Research, Air Research Development Command, U. S. Air Force.
† Now at Palmer Physical Laboratory, Princeton University, Princeton, New Jersey.
[1] See A. Dauvillier, Cahiers phys. No. 35/36, 1 (1951) for a comprehensive review of all published studies through 1950.
[2] H. Elliot, *Progress in Cosmic Ray Physics* (Interscience Publishers, Inc., New York, 1952), p. 455.
[3] Forbush, Gill, and Vallarta, Revs. Modern Phys. **21**, 44 (1949). See also references 1 and 2.
[4] J. A. Simpson, Phys. Rev. **83**, 1175 (1951) and references therein. See also Phys. Rev. **73**, 1389 (1948).
[5] J. A. Simpson, Proceedings of the Echo Lake Conference no Cosmic Rays, p. 175, U. S. Office of Naval Research, Dept. of Navy, June, 1949.
[6] J. A. Simpson, Phys. Rev. **81**, 895 (1951).
[7] N. Adams and H. J. Braddick, Z. Naturforsch. **6a**, 592 (1951).

observe changes of spectrum with time. Specifically, we wish to determine, (a) to what extent the sun is important for our understanding of the origin of intensity variations, and (b) what kinds of accelerating processes are required to account for the observed variations. Thus, we desire not only the dependence of primary radiation intensity with *time* but also the *energy dependence* of these variations. For measuring intensity variations of primary particle momenta greater than the equatorial geomagnetic cutoff, an artificial cutoff such as absorption may be employed. For lower momenta the magnetic field of the earth is available for momentum selection, and, in this geomagnetic latitude sensitive region of the primary spectrum, we measure the intensity variations of the component with the largest latitude dependence.

Since intensity variations are produced by acceleration, injection, or perturbation processes, it is clear that an extension of our knowledge of intensity variations will have a bearing on the origin of cosmic-ray particles, perhaps limited to the origin of the most intense low momentum region of the primary spectrum.

We shall be concerned in this paper with the problems of (a) the use of the nucleonic component for intensity variation determinations, (b) examining the quantitative problem of relating secondary component intensity measurements deep in the atmosphere to the primary variations, (c) determining the influence of the terrestrial atmosphere upon intensity variations, and (d) the design and operation of a series of detectors at selected geomagnetic latitudes for experimental purposes.

Before proceeding further, however, we wish to define the fundamental groups of intensity-time variations which we may observe.

II. DEFINITIONS OF COSMIC RADIATION INTENSITY VARIATIONS

Observed variations of intensity with time depend both upon the location of the observer and the physical phenomena producing the variations. For clarity in future discussions on this subject we shall define kinds of intensity variations from the point of view of phenomenological concepts rather than from the analytical methods often used to study variations. For example, a twenty-four hour intensity cycle which recurs for, say, 0.3 to 0.5 of a total observing period of many days may be averaged over the entire period and, therefore, over days of no variation. The amplitude of an harmonic function may be computed to describe the mean or average variation. Clearly this description has become dependent on the analytical method used. From the latter point of view this is a variation occurring *every* day (diurnal) with given average amplitude; from the phenomenological point of view this variation is a recurring or intermittent phenomenon. Intuitively, we expect that the phenomenological descriptions may

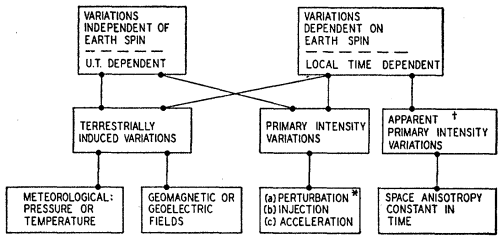

FIG. 1. The phenomenological classification of intensity *vs* time variations and their origins. Possible variations which are a function of the orbital motion and axis tilt of the earth are not included. Thus, this chart represents the classes of intensity *vs* time variations for which the periods of variation are less than the order of 100 days. * If induced by solar processes, this is the solar cosmic radiation component. This includes the solar flare effect. † For example, a variation which depends upon the angle included by the primary particle trajectory and the velocity vector of the solar system with respect to the galaxy.

contribute to progress on a satisfactory theory for the origin of the variation.

Since all observations are made near the surface of the earth under both an atmosphere and a varying geomagnetic field a natural dichotomy of intensity variations exists; namely, a division of all variations into (1) those of terrestrial origin and (2) those of primary cosmic radiation origin. Because of the spin of the earth any anisotropy of the primary radiation is detected by a local observer as an intensity variation which is a function of *local* time, e.g., sidereal or solar mean time. For the special case where the intensity of the anisotropic distribution is constant in universal time (G.M.T.) we call this an *apparent primary intensity variation* in the observer coordinates. All other intensity variations in division (2) above are defined as *primary intensity variations*.

Primary intensity variations dependent on the axial spin of the earth are called either (a) *recurring daily variations* if the variations persist for only a few consecutive days and reoccur at a later time,[8] or (b) *diurnal variations* if the daily variations occur *every* day.

If the acceleration or perturbation processes producing primary intensity variations occur in the region of the sun and are related to solar phenomena, we call these related intensity variations the *solar component* of the primary cosmic radiation intensity.[9] The solar flare effect[3] is an infrequent phenomenon in the solar component.

The classes of intensity variations have been related in Fig. 1 from the position of the local observer coordinates shown in Fig. 2. For reference, the solar spin and both earth axial and orbital spin directions are shown with respect to the local observer coordinates.

Terrestrially induced intensity variations, on the other hand, may be subdivided into two types: (1) those

[8] Fonger, Firor, and Simpson, Bull. Am. Phys. Soc. **27**, No. 5, 6 (1952).
[9] Simpson, Fonger, and Wilcox, Phys. Rev. **85**, 366 (1952).

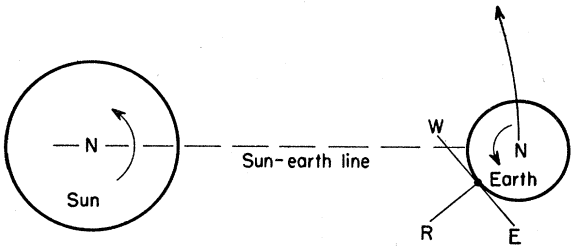

FIG. 2. The local coordinates of a detector at $\lambda=0°$ is shown with respect to the sun-earth line and the relative motions of the two bodies. W=west; E=east; R=radial or "vertical" direction.

of meteorological origin and (2) those arising from changing magnetic or electric fields in the region of the earth. These are effects which interfere with the study of primary variations. Since it is well established that many meteorological and magnetic field effects are associated with solar phenomena, it is particularly important to understand their effect on secondary radiation intensity. Clearly solar effects in the terrestrial atmosphere do *not* represent a solar component.

III. THE CHOICE OF THE NUCLEONIC COMPONENT NEUTRONS FOR OBSERVATION

Since the low energy nucleonic component possesses the largest known geomagnetic latitude effect, we shall summarize briefly the properties of this component in so far as they pertain to the study of intensity variations. Primary particles interact with air nuclei to yield secondary high energy mesons, nucleons and fragments. These secondary particles generate by collision processes in the atmosphere a cascade or chain composed principally of nucleons. As the cascade degenerates in total energy the composition of the cascade becomes almost entirely nucleons of <1 Bev/c. The degradation of nucleon energy continues through collision and capture processes which are recognized as nuclear disintegrations or "stars." See Fig. 3. At atmospheric depths sufficient for the nucleon flux and star production to be in equilibrium ($x>200$ g-cm^{-2}), each nuclear disintegration yields on the average several protons and neutrons having energies in the range $\sim$1–20 Mev. These low energy nucleons are called disintegration product nucleons; the protons rapidly lose energy by ionization, and the neutrons are reduced in energy by N and O collisions to become the slow neutrons in the atmosphere.[10] In summary, a primary particle of given momentum at the top of the atmosphere is related to low energy stars at an atmospheric depth x by a cascade or chain of nucleons.

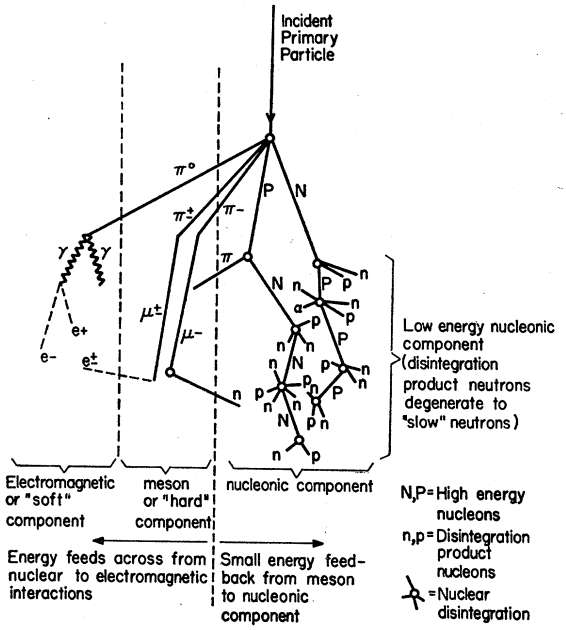

FIG. 3. Schematic representation of the typical development of the secondary cosmic radiations within the atmosphere arising from an incident primary particle. Additional secondary interactions which lead to neutron production are shown in Fig. 13.

The disintegration product neutrons and slow neutrons in the atmosphere are produced predominantly by the nucleonic component since, for example, neutron yields from γ-n, π-star-n, μ-star-n, and similar processes are small, but the nucleon-induced disintegrations have large cross sections and yield, on the average, more than one neutron per disintegration. From the experimental point of view it is more convenient, reliable, and precise to use neutron detectors rather than the ionization from nuclear disintegrations to measure the properties of this low energy component. Hence, we measure the disintegration product neutron intensity to observe temporal changes of nucleonic component intensity.

Even though the high energy star producing nucleon flux is peaked in the vertical direction within the atmosphere, the disintegration product neutrons are emitted almost isotropically from nuclei and scattered. Consequently, an omni-directional neutron detector such as a boron trifluoride proportional counter measures the neutrons produced within a small volume of the atmosphere surrounding the detector. Thus, reported measurements of neutron intensity in the atmosphere are for isotropic distributions.

We now return to the discussion of the low energy nucleonic component and neutron latitude effect in the atmosphere. Figure 4(a) presents a comparison of the shielded ion chamber,[11] the vertical counter telescope,[11] and the neutron latitude dependence at constant atmospheric depth $x=312$ g-cm^{-2}. The data are assigned unit intensity at $\lambda=0°$. In Fig. 4(b) these data have been represented on a log scale as curves B and B' along with the neutron latitude curve C at $x=500$ g-cm^{-2} (approximately 11 000 ft) and the shielded ion chamber at sea level D.[12] At atmospheric depths down

[10] Bethe, Korff, and Placzek, Phys. Rev. **57**, 573 (1940).
[11] Biehl, Neher, and Roesch, Phys. Rev. **76**, 914 (1949).
[12] E. B. Berry and V. F. Hess, Terr. Mag. Atmos. Elec. **47**, 251 (1942).

to $x \approx 500$ g-cm^{-2} the absorption mean free path (m.f.p.) for the star producing radiation has been shown to be a function of λ, *i.e.*, a function of the average primary radiation energy.[4] Moreover, it has recently been found that $x > 500$ g-cm^{-2} the values for L all approach a constant value *independent* of latitude.[13] [See Sec. VIII(b).] Thus, the neutron latitude curve C also represents closely the sea level latitude dependence and should be compared with the corresponding sea level ion chamber curve D. From these facts we conclude that a large neutron latitude effect is to be found even at sea level and that the neutron component most closely fulfills the conditions for studying low energy primary intensity variations. It will become clear in the following sections that there are many additional factors which favor the choice of the neutron component monitor for measuring low primary energy intensity variations.

IV. THE RELATIONSHIP BETWEEN NEUTRON CHANGES IN THE ATMOSPHERE AND CHANGES OF PRIMARY PARTICLE INTENSITY

Having selected the neutron component intensity as most closely fulfilling our requirements for studying temporal variations, we investigate the problem of relating the observed neutron intensity changes at atmospheric depth x to the changes of primary particle intensity taking into account the composition of the primary radiation. We first consider the relationship between the neutron and primary radiation intensities. Clearly, it is difficult to calculate for a primary nucleon of given momentum the expected yield of neutrons at position λ, x in the atmosphere without knowing cross sections for high energy meson and nucleon production, details of charge exchange and other facts which are a prerequisite for calculating the behavior of the nucleonic component. Hence, we take a phenomenological approach to the problem and derive a functional relationship between observed neutron intensity and primary particle momentum based on the facts that the primary momentum spectrum for protons, alpha-particles, and heavier nuclei and observations of neutron intensity as a function of λ,x are now fairly well known. (We neglect, for the present, discussion of the longitude dependence.)[14,15] More precisely, we define the *specific yield* of neutrons as a function $S_Z(N, x)$ which gives the observed time-averaged counting rate at depth x arising from a unit flux of vertically incident primary particles of charge Z and momentum-to-charge ratio (magnetic rigidity) $P/Z \equiv N$. We call $j_Z(N, t)$ the differential spectrum for primary particles of charge Z at time t.

[13] J. A. Simpson and W. Fagot, Phys. Rev., to be published.

[14] Winckler, Stix, Dwight, and Sabin, Phys. Rev. **79**, 656 (1950); B. Peters, *Progress in Cosmic Ray Physics* (North Holland Publishing Company, Amsterdam, 1952); H. V. Neher, Phys. Rev. **83**, 649 (1951); M. L. Vidale and M. Schein, Nuovo cimento **8**, 774 (1951).

[15] S. B. Treiman, Phys. Rev. **86**, 917 (1952); thesis, University of Chicago, 1952, unpublished.

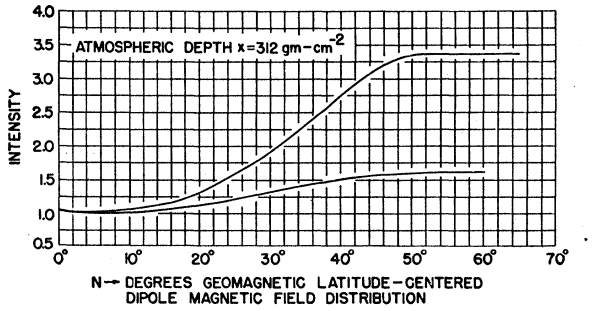

FIG. 4. (a) The lower curve represents the latitude dependence for either an unshielded ion chamber or vertical counter telescope with no absorber. (See reference 11.) The upper curve represents the disintegration product neutron production also normalized to $I=1$ at $\lambda=0°$. (See reference 4.) The data for both curves were obtained in June, 1948.

S_Z and j_Z are expressed as functions of momentum-to-charge ratio rather than energy because the trajectories for charged particles in a static magnetic field are uniquely determined by P/Z.

For particles of given rigidity N, certain directions of arrival at the earth may be forbidden, in the sense that particles coming from infinity cannot approach the earth from these directions because they are

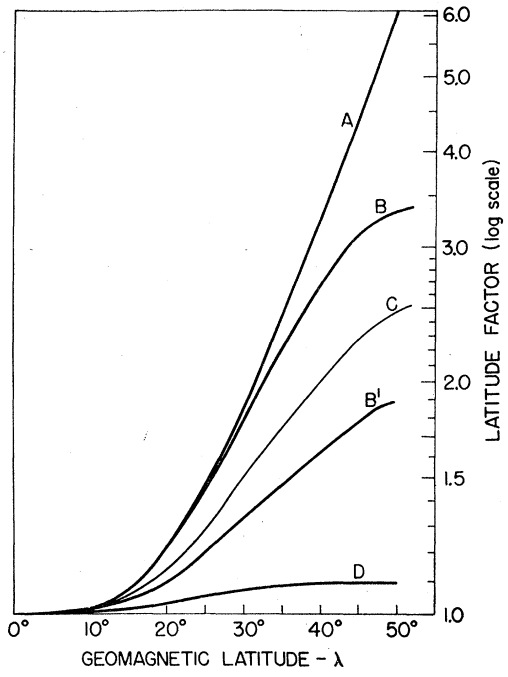

FIG. 4. (b) The latitude factor of intensity increase above $\lambda=0°$ is shown on a log scale. Curve A represents the primary integral spectrum of the protons plus nuclei $Z>1$. Curves B and B' are the intensity of fast or slow neutrons (B) and the ion chamber (B'), respectively, as shown in Fig. 4(a) at $x=312$ g-cm^{-2}. Curve C gives the latitude factor for fast neutron production at $x=680$ g-cm^{-2} (11 000 ft). As shown in Sec. VIIIa, this curve remains essentially unchanged down to sea level. Curve C for neutron production may, therefore, be compared with Curve D for a shielded ion chamber at sea level. (See reference 12.)

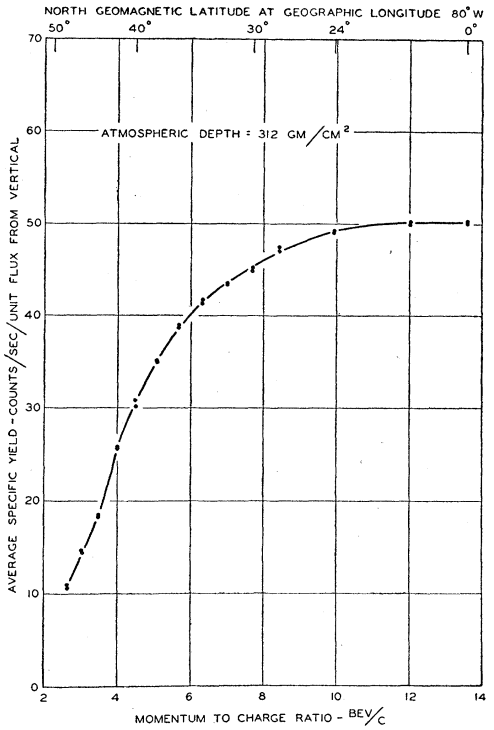

FIG. 5. The average specific yield of neutrons from the vertically incident mixed primary radiations (derived from 1948 data).

deflected in the terrestrial dipole field. Vallarta[16] distinguishes a *main cone* within which all directions of arrival are allowed, and the *Stoermer-plus-shadow* cone outside of which all directions are forbidden. Between the two limiting cones is a region called the *penumbra* which contains an infinite number of allowed and forbidden subregions. The shapes of these cones depend not only on N but also on magnetic latitude λ. In other words: for arrival from a given direction at a given latitude, one can distinguish two limiting values of N. Below N_1 all rigidities are forbidden, above N_2 all rigidities are allowed, and between N_1 and N_2 there are an infinite number of allowed and forbidden subregions.

At the equator there is no penumbra, and the allowed cone coincides with the main cone. At high latitudes the penumbra consists mainly of allowed regions, so that the allowed cone is determined chiefly by the Stoermer-plus-shadow cone. Thus, at very high and very low latitudes one can assign (approximately) a unique cut-off value of N, above which all rigidities are allowed and below which all are forbidden. At intermediate latitudes ($\sim 20°$–$30°$) the penumbra is complex, but even here it is sufficiently accurate for many purposes to assign a unique cut-off rigidity for arrival from any given direction.[17] Within these limitations then, we shall assume a unique cut-off rigidity $N(\theta, \varphi, \lambda)$ for arrival of particles from zenith angle θ and azimuthal angle φ at magnetic latitude λ.

It follows from the earlier definition of specific yields, therefore, that the total counting rate $R(\lambda, x, t)$ of a neutron detector located at depth x, latitude λ, and time t is given by

$$R(\lambda, x, t)=\sum_Z \int^{2\pi} d\varphi \int_0^{\pi/2} \sin\theta d\theta \times \int_{N(\theta,\varphi,\lambda)}^{\infty} S_Z\left(N, \frac{x}{\cos\theta}\right) j_Z(N, t) dN. \quad (1)$$

Since the detector is omni-directional, the counting rate due only to those primary particles which arrive from the vertical direction per unit solid angle, and which we refer to as the "vertical" counting rate R_v, is

$$R_v(\lambda, x, t)=\sum_Z \int_{N_v(\lambda)}^{\infty} S_Z(N, x) j_Z(N, t) dN, \quad (2)$$

where $N_v(\lambda)$ is the cut-off rigidity for vertical arrival. At large atmospheric depths, R_v and R are related in very good approximation by the Gross transformation[15]

$$2\pi R_v = R[1+x/L], \quad (3)$$

where $1/L=-R^{-1}(dR/dx)$. As noted in the previous section, L will in general depend on x and λ.

It is clear from the above discussion that R, j, and N are to be measured simultaneously. In fact, this is only partially true; R and j are time averaged values.

(a) Properties of the Specific Yield Functions

From Eq. (2) we obtain the relationship

$$dR_v/d\lambda = -\sum_Z S_Z(N_v, x) j_Z(N_v)(dN_v/d\lambda), \quad (4)$$

at time t. In the range $\sim$3–15 Bev/c the spectra of the various species of primary particles are fairly well known,[14] and they are well represented by a power law of the form $j_Z=K_Z N^{-2.0}$. With the aid of Eq. (4) some properties of the specific yield functions can be determined from a knowledge of the primary spectra and of the latitude variations for neutron production in the atmosphere. We summarize here the pertinent results of such a study.[15]

(1) For atmospheric depths between at least 200 and 600 g/cm^2 the specific yields (expressed now as a function of energy rather than rigidity) become energy-insensitive in the range $\sim$4–13 Bev/nucleon—for all species of primaries; and this insensitivity probably extends up to considerably higher energies.

(2) In the energy-insensitive region the specific yields vary with depth x (for $600>x>200$ g/cm^2) in an approximately exponential manner, with mean free path 270 g/cm^2.

[16] M. Vallarta, *On the Allowed Cone of Cosmic Radiation* (Toronto University Press, Toronto, 1938).

[17] See, e.g., L. Janossy, *Cosmic Rays* (Oxford University Press, London, 1948), Chap. VII.

(3) At energies much below 4 Bev the specific yields fall off rapidly with decreasing energy, this effect becoming more pronounced with increasing depth.

(4) In crude approximation, at a given per-nucleon energy the specific yield of a heavy primary particle is larger than that of a proton by a factor A, where A is the number of nucleons in the heavy particle.

In Fig. 5 the *average* specific yield $S(N, x)$ for the mixed primary particle radiation is plotted as a function of rigidity for atmospheric depth 312 g/cm², where

$$S(N, x)=[\sum_z S_z(N, x) j_z(N)]/[\sum_z j_z(N)], \quad \text{at time } t. \quad (5)$$

The specific yield function at 680 g-cm^{-2} (11 000 ft mountain stations) may be computed using curve C in Fig. 4(b).

(b) Specific Yield of Neutrons from Primary Protons

In Fig. 6 the *proton* specific yield at 312 g/cm² is plotted as a function of primary *proton* kinetic energy. Both curves (Figs. 5 and 6) are based on the total primary spectrum given by Winckler *et al.*[14] Although these curves may be fairly precise at high energies, they are uncertain at low energies (low rigidities) because the shape of the total primary spectrum curve at low rigidities appears to be in doubt. During "quiet" periods, the neutron latitude curves flatten out for latitudes above the "knee" at $>52°$.[4] This means either: (1) the flux of primary particles with N smaller than $N_v(52°)\approx 2$ Bev/c is very small; or (2) the specific yields for $N<2$ Bev/c are very small, i.e., the low energy particles do not produce secondary events that reach large atmospheric depths. The curves of Figs. 5 and 6 reflect the choice of explanation (2), since the Winckler spectrum indicates the presence of appreciable numbers of particles with $N\lesssim 2$ Bev/c. This is also supported by the high latitude balloon flights of

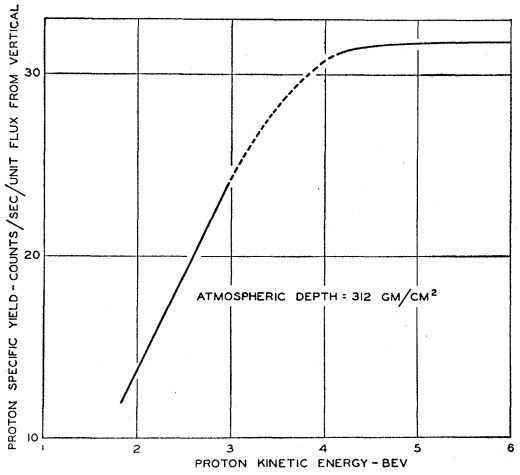

FIG. 6. The neutron specific yield from vertically incident primary protons.

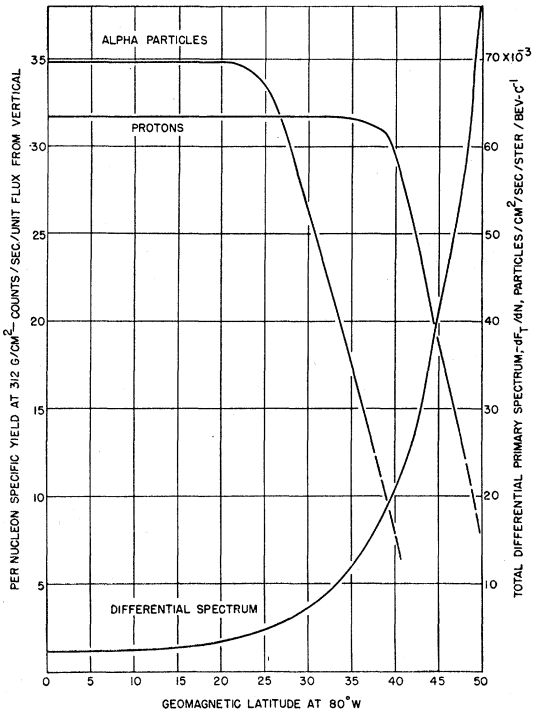

FIG. 7. The specific yields *per* nucleon for vertically incident alpha-particles or protons (see Sec. IV).

Pomerantz.[18] However, the recent extensive balloon experiments of Neher[19] indicate that no new particles arrive at latitudes above at most 56°. Furthermore, the 1949 event[20] in which the neutron intensity at 312 g/cm² increased and the "knee" of the latitude curve moved up to 56° indicates that the low energy primaries corresponding to the latitude interval 52°–56° *can* contribute to neutron production at large depths. This suggests that during "quiet" periods the flux of low energy primaries (with energies below that corresponding to 52°) is small, but that new low energy primaries may occasionally arrive at the top of the atmosphere during "disturbed" periods, their specific yields being nonvanishing down to energies corresponding to at least 56°.[20a]

(c) Specific Yield of Neutrons from Primary Alpha-Particles

We now compare the specific yields for a primary nucleon which arrives free (proton or neutron) at the top of the atmosphere and a primary nucleon of the same energy which arrives bound in a heavy particle. Since over 90 percent of the nucleons in the primary radiation[14] are carried in the proton and alpha-particle

[18] M. A. Pomerantz, Phys. Rev. **77**, 830 (1950).
[19] H. V. Neher and E. A. Stearn, Phys. Rev. **87**, 240 (1952).
[20] J. A. Simpson, Phys. Rev. **81**, 639 (1951).
[20a] *Note added in proof.*—The above results are for 1948. Our studies of neutron latitude curves for 1950–1951 now show conclusively that the curves become flat above $\lambda\approx 55°$–56°. These changes in cutoff appear to be real.

flux we neglect, for the present, the contribution of nucleons by heavier nuclei. We assume that the binding of a nucleon in a nucleus is not important in collisions between nuclei at high energy and that an alpha-particle breaks up completely into nucleons in its first collision in an air nucleus. Although there is little experimental evidence on this latter assumption it appears reasonable since the probable heavy fragments of the breakup have low binding energies. We find that

$$S_\alpha(E, x)/S_p(E, x)=1.1\times 4=4.4$$

using the above assumptions.

In Fig. 7 the function $S_p(N, x)$ and $S_\alpha(N, x)$ per nucleon have been plotted as a function of geomagnetic latitude λ, where $N=N_v(\lambda)$ is the cut-off rigidity at λ.

(d) Intensity Variations

In discussing variations of primary cosmic-ray intensity measured by a neutron detector, we shall use the pair of Eqs. (2) and (3) rather than the more complicated, but more appropriate, Eq. (1). Note that the so-called "vertical" counting rate is not measured experimentally; it is deduced from the experimentally measured values of R and its logarithmic slope. Now assume that at a given location, R and L change by δR and δL, respectively, where the variations are considered to be small. From Eq. (3) we find for the fractional change in "vertical" counting rate

$$\frac{\delta R_v}{R_v}=\frac{\delta R}{R}-\frac{x/L}{1+x/L}\cdot\frac{\delta L}{L}. \tag{6}$$

From Eq. (2) we see that a change in the cosmic-ray intensity below the top of atmosphere may come about in any one (or combination) of several ways:

First, the change may be due to variations in the primary cosmic radiation far from the earth, i.e., variations in the absolute magnitudes or rigidity dependencies of the spectra $j_Z(N)$.

Second, the counting rate will depend on meteorological factors such as the temperature or pressure distribution in the atmosphere.

Third, even if the primary spectra far from the earth are unchanged, the flux of particles which arrives at the earth may vary because of changes in the cut-off rigidity. For example, this could occur as a result of perturbations in the terrestrial magnetic field. More generally, we recall that the assignment of a unique cut-off rigidity for arrival from a given direction is only an approximation, even in the field of a simple dipole. Actually, between the two limiting rigidities N_1 and N_2 there is the penumbra region. In general, field perturbations might be expected to change not only the size of the penumbra region but also the density of allowed subregions within the penumbra.

In the remainder of this section we will make some general remarks on changes of the types (1) and (3) discussed above, without going into details of the observational data on time variations.

(e) Variations of Primary Cosmic Radiation Intensity

We consider here the case where the variations in measured neutron intensity below the top of the atmosphere are due to changes in the primary radiation. For an event of this kind we can make the following general observation. From Eq. (4) it is clear that a change in the *slope* of the R_v-latitude curve at any latitude λ represents a change in the flux of primaries having rigidity equal to the cut-off value at λ.

As mentioned in part (c) the heavy particle and proton specific yields can be expected to show roughly similar dependencies on (per-nucleon) energy (except for a constant factor), and at low energies ($\lesssim$4 Bev) the specific yields fall off rapidly with decreasing energy. But for a given rigidity, a heavy primary particle (mass-to-charge ratio$\approx$2) has a smaller per-nucleon energy than a proton. It then follows from Eq. (4) that with increasing latitude (at high latitudes), the proton primaries become increasingly more important than the heavy primaries in contributing to the *slope* of the neutron latitude curves. This is shown in the specific yield curves of Fig. 7. Thus, any change in the slope $dR_v/d\lambda$ above 43° would essentially reflect only the change in the proton spectrum:

$$(\lambda\gtrsim 43^\circ)\quad \frac{dR_v'/d\lambda}{dR_v/d\lambda}=\frac{j_p'(N_v, t')}{j_p(N_v, t)}. \tag{7}$$

(The primed and unprimed quantities refer to two different times.)

(f) Variations of Magnetic Cut-Off Rigidity

Irrespective of the reasons for the flattening of the neutron latitude curves above the "knee" at $\sim$52°–56°, we can state the following. To the extent that the latitude curves are truly flat above the "knee," no change in the cut-off rigidities, i.e., no magnetic perturbations, can account for an *increase* or *decrease* in neutron intensity above the "knee": A decrease in the cut-off rigidity at any latitude permits new, lower energy particles to arrive at that latitude; but the very existence of the "knee," as we have seen, implies either that the lower energy particles are not present in the primary radiation or that the lower energy particles do not contribute to neutron production at the detector position λ, x. Recent measurements by Van Allen indicate that the low energy primaries are not normally present.[21]

The cut-off rigidity, e.g., for vertical arrival, is a function of latitude and also of the parameters describing the magnetic field (e.g., the earth's dipole

[21] J. A. Van Allen, private communication.

moment, in the case of a simple dipole field, and additional parameters when perturbing fields are present). Let q be one such parameter, and suppose that it undergoes a small variation δq. We have the relationships $R_v=R_v(N_v)$ and $N_v=N_v(\lambda, q)$, from which it follows that

$$\delta R_v=\left[\frac{\partial R_v}{\partial \lambda}\right]\left[\frac{\partial N_v/\partial q}{\partial N_v/\partial \lambda}\right]\delta q. \tag{8}$$

The above arguments hold not only for neutron detectors but for cosmic-ray detectors of any kind. The response of any detector to magnetic perturbations is seen to depend on the slope of the latitude curve. Since, as we have shown in Sec. III, the nucleonic component has the largest latitude effect of any secondary component of the cosmic radiation, it is the most suitable component for detecting the effects of magnetic perturbations on the cosmic radiation as well as for studying primary temporal variations of intensity.

V. THE LOCAL PRODUCTION OF NEUTRONS

The measurements of neutron intensity as a function of λ, x and the analysis of the neutron specific yields from primary radiations all refer to neutrons produced in the free atmosphere, i.e., disintegration product neutrons from N and O nuclear disintegrations. The neutrons are detected by a BF_3 proportional counter with either the atmosphere as the neutron energy moderating medium (a slow neutron measurement) or by using a local condensed moderating material such as paraffin or carbon surrounding the detector (a fast neutron measurement). The latter kind of detector avoids the atmosphere as a moderator and thus reduces or eliminates the difficulties which arise from changes in air moderator characteristics in the region of clouds, during precipitation, etc. This was the principal reason for measuring the neutron distribution as a function of x, λ with a fast neutron detector.[4] However, when this detection method is applied to continuously monitored neutron production in the atmosphere several difficulties arise. First, the detector responds to changes of ambient neutron production near the detector owing to movement of heavy materials, snowfall, personnel, and neutron emitting radioactive sources. Second, for a given quantity of BF_3 gas the observed counting rate is relatively low.

These difficulties are in large measure eliminated by requiring that the detected neutrons originate in locally produced stars from condensed materials. We define this process as *local neutron production*. The neutron production in elements is a function of atomic weight. The average number of neutrons emitted by a low energy nuclear disintegration is called the multiplicity, ν; the ratio of neutron multiplicity from lead to carbon is $\sim 8:1$ as determined from both low altitude[22,23] and high altitude measurements up to ~ 200 g-cm^{-2}.[24] It is clear that by using materials of large A mixed with a local neutron moderator, we exclude the atmosphere and the environment of the detector as both the neutron source and moderating medium, while, on the other hand, the neutron yield has been increased. We shall call a detector of the above type a local production geometry or a *pile geometry*. Specific designs will be discussed in Sec. VI.

If we wish to apply this type of detector to the problems outlined in the earlier sections of this paper, we must know the specific yield function $S(\lambda, x)$ to be used with a local producer. Namely, we determine to what extent the properties of the low energy nucleonic component discussed earlier may be extrapolated to local neutron production in a pile. To investigate this problem, elementary pile structures have been transported in aircraft to measure local production as a function of atomic weight A over the latitude range 0° to 65° and at atmospheric depths below 200 g-cm^{-2}.[4,24] We shall only summarize the general results here. The measurements show a latitude and altitude agreement with free atmosphere measurements within ~ 6 percent. An exception occurs in the latitude range $\lambda > 38°$ where differences in the altitude dependence between carbon and lead are found for small x. In general, there appears to be remarkably good agreement, however, between local and free air neutron production if low energy nuclear processes are measured. The latitude dependence for local production of small nuclear disintegrations measured in a pulse ion chamber also agrees closely with neutron production.[25] The behavior of local production is discussed in Sec. VIII(a) for large atmospheric depths.

From the high altitude measurements it has also been determined that at $\lambda = 52°$ the local neutron production from showers, π and μ mesons, and γ-produced stars is less than 3 percent of the total incoherent neutron production. Background pulses from counter contamination, recoil events, and star production in gas and walls are less than 1 percent of the total count rate.

It is clear from the above summary that for $x > 200$ g-cm^{-2} not only is the observed counting rate in a local production geometry nearly proportional to free air measurements but the detector is insensitive to secondary radiation in the electromagnetic or meson component. Hence, unless we state otherwise, we shall apply the specific yield functions of Sec. IV to local neutron production in pile geometries.

VI. PILE GEOMETRIES FOR LOCAL NEUTRON PRODUCTION AND BASIC INSTRUMENTATION

(a) Pile Parameters

We now examine the design problems for a local neutron geometry suitable for continuous observation of intensity changes of local neutron production by the

[22] V. Tongiorgi, Phys. Rev. **76**, 517 (1949).
[23] C. G. Montgomery and A. R. Tobey, Phys. Rev. **76**, 1478 (1949).
[24] J. Simpson, Proc. Echo Lake Cosmic-Ray Symposium, U. S. Office of Naval Research, Dept. of Navy, p. 252 (1949).
[25] Simpson, Baldwin, and Uretz, Phys. Rev. **84**, 332 (1951).

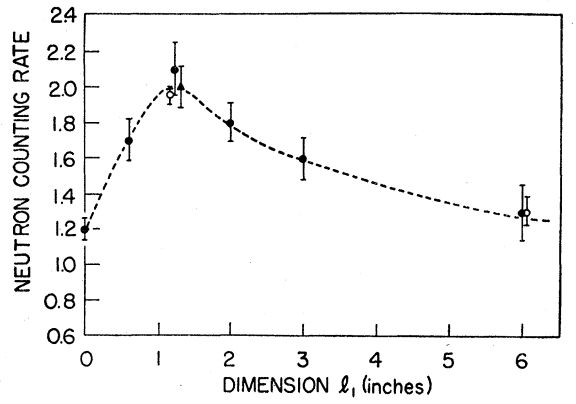

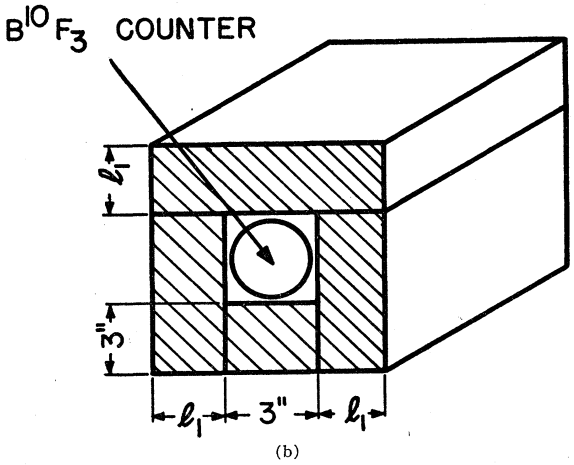

FIG. 8. The optimum thickness of paraffin for moderating disintegration product neutrons was approximated by measurements with the geometry shown in Fig. 8(b) (see Sec. VI).

nucleonic component. Elementary geometries were studied in this laboratory[24] in 1948 and 1949 principally for measurements in aircraft. Geometries for the study of local neutron production have also been reported by Cocconi, Tongiorgi, *et al.*,[22,26] Montgomery[23] and recently by Adams and Braddick.[7] Since several geometries were to be constructed for our experiments we decided upon a relatively simple design which is easily reproduced. Lead is used for local star production. The selection of the neutron moderating medium reduces to a choice between paraffin and carbon. Aside from the smaller local neutron production in paraffin, paraffin was selected since it is conveniently prepared in any required geometrical form. To further simplify construction, the geometry was limited to rectangular elements.

Since the energy distribution of the locally produced neutrons from stars in lead is not known we determine by experiment the optimum moderator thickness l_1, as defined in Fig. 8, for detection by a BF_3 proportional counter. Locally produced neutrons from lead were moderated with the simple geometrical arrangement shown in Fig. 8(b). It is clear that approximately 1.25 inch represents the optimum value for l_1 between local producer and counter. The lead thickness l_2 was arbitrarily determined from the requirement that l_2 be greater than the local transition maximum in lead.[27] $l_2 \approx 2$ inches was selected so that attenuation of the incident nucleon intensity would not be large.

The third design parameter was concerned with the disposition of additional moderating and scattering paraffin to surround the lead-paraffin-counter geometry. The thickness l_3 of this paraffin was determined emperically using a radium-beryllium source to reduce the detection of neutrons produced *outside* the geometry. Each increase of l_3 by $\Delta l_3 = 1.5$-inch paraffin reduced the detected neutrons from the source by a factor ~ 2. When the amount of paraffin required in a practical geometry is considered the attenuation leads to a practical value of $l_3 \approx 6$ inches; this is more than the required thickness for moderating and scattering the neutrons produced in the lead.

The length of the pile geometry l_4 was determined by the BF_3 counter design described in part (c) below. By taking account of the paraffin end layers, an over-all pile length of $l_4 = 46$ inches was obtained.

A simple pile design was derived from these four dimensions; l_1, l_2, l_3, and l_4. To increase the counting rate and decrease the lead requirements two counters were used with the lead cross section in the form of an "I" as shown in Fig. 9. The dimensions were adjusted to utilize standard 1 lb "parowax" blocks and 2×4×8 in. extruded lead blocks. Thus, the pile may be dismantled for transportation purposes. We call this design a "standard" since it may be constructed anywhere from detailed specifications, and for a given x, λ, t all piles will agree within ~ 5 percent.

The basic pile design may be extended to N counters

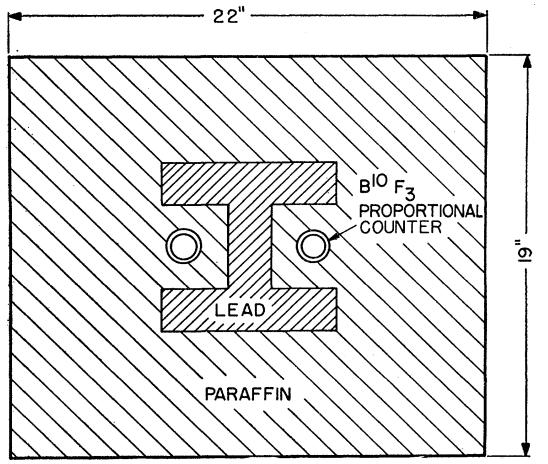

FIG. 9. Cross-section view of the "standard" pile used at some of the observing sites given in Table II. This geometry may be readily reproduced for comparison with the measurements reported in this paper.

[26] Cocconi, Tongiorgi, and Widgoff, Phys. Rev. **79**, 768 (1950).

[27] S. B. Treiman and W. Fonger, Phys. Rev. **85**, 364 (1952).

by adding horizontally additional lead "I" units. Since the incident nucleons are strongly peaked in the vertical direction, the counting rate increases approximately linearly with the number of counters. A pile composed of 12 counters is shown in Fig. 10.[28] The time constant of the paraffin-lead pile is approximately 175 microseconds for e^{-1} decrease of neutron density.

(b) Origin of the Pile Neutron Counting Rate

Using the basic two-counter pile we examine the origin of the neutrons in the pile. The counting rates with and without the lead local neutron producer show that 84 percent of all the detected neutrons are produced in the lead. The remaining 16 percent is divided approximately among production in paraffin (carbon) ~13 percent; and counter background plus neutrons entering from outside the geometry, ~3 percent. These were observations from the two-counter piles at Chicago, Climax, and Huancayo. The results are tabulated in Table I. It is clear from Table I that the local neutron production properties of this pile design are reproducible.

(c) BF_3 Proportional Counters

The BF_3 counters are designed to operate with an applied potential difference of approximately 2000 volts so that the high potential system may be used in field stations under widely varying local conditions without introducing spurious pulses. With this restriction the counters were filled with BF_3 enriched to 96 percent boron-10 at 45 cm Hg pressure. The important dimensions are

Active length	=34 in.
Diameter	=1.5 in.
Center wire diameter	=0.001 in.

The curve for counting rate *vs* applied potential has almost zero slope over a range of 200 volts.

It is essential to use counters with constant, low background count rates. A typical background rate at sea level with the counter surrounded by cadmium is 1.5 counts per minute. The problem of maintaining a constant counter background for piles operated at sea level is particularly important owing to the low level production rate at sea level. The counters appear to have an indefinitely long lifetime if the gas is properly purified.

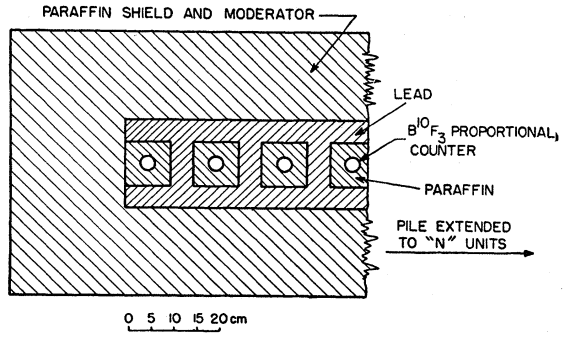

FIG. 10. The pile extended to 12 counters is used as the detector at Chicago and Climax (11 000 ft). This pile is composed of 6500-lb lead plus approximately 3000 lb paraffin. Cross-section view.

[28] This pile design requires 6500 lb lead and 3000 lb paraffin.

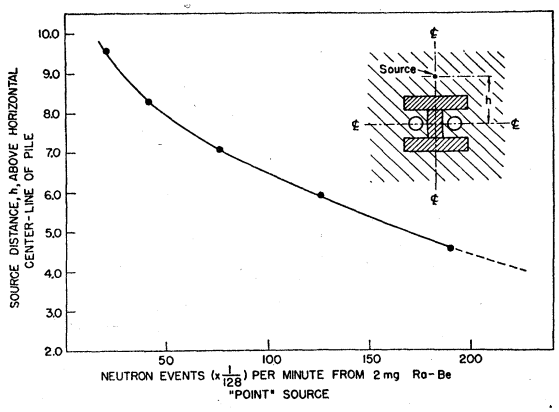

FIG. 11. Source position along vertical center line within the standard pile (Fig. 9) *vs* recorded neutron intensity. These data determine the selection of an appropriate position within the pile for a Ra-Be neutron source for normalization of the detector (see Sec. VId).

(d) Normalization of Pile Count Rate to Ra-Be Point Source

Clearly the local production in lead represents a distributed source of neutrons. We are restricted, however, to a Ra-Be neutron source which approximates a point source whenever a test source is required. The Ra-Be source may be inserted at selected positions in the pile[29] to check the over-all performance of the detector and recording equipment. The neutron count rate as a function of point source position is given in Fig. 11.

The Ra-Be source does not calibrate a series of piles. Calibration is best achieved by the intercomparison of all pile structures under identical cosmic radiation conditions.

(e) Stability of the Detection System

The parallel connected proportional counters are coupled to a negative feedback pulse amplifier. Pulses from the amplifier output are selected by a discriminator circuit which also provides the correct pulse shape for the scaling circuit. The integral count is recorded by a register which is photographed along with a sensitive dial pressure indicator, thermometer and chromometers at predetermined intervals. The scaler pulses also operate a counting rate computer which records on a log scale individual points of predetermined probable error; this computer system is used at four observing

[29] Thimbles which extend into the pile are provided for inserting a Ra-Be source.

TABLE I. Origin of the neutron counting rate within a standard 2-counter lead and paraffin pile.

Neutron count rate origin	Chicago	Climax	Peru
Lead	82%	85%	83%
Paraffin+counter background+environment	18%	15%	17%

stations to record sudden increases of radiation intensity.

By dividing the 12-counter pile (Fig. 10) into two 6-counter units each with independent electronic systems the performance of the system can be checked by comparing the count rates of the two half systems. This procedure is used at Chicago and Climax.

The stability of the electronic system for continuous operation is improved by reducing the gain of the two amplifier feedback loops to ~ 20 each. The aging characteristics of the discriminator circuit are such that the threshold for pulses tends to *decrease* with time, whereas the amplifier gain tends to decrease with time; this compensation produces an input pulse sensitivity which is stable for long periods of time. Since the high voltage supply is constant within ± 10 volts and the proportional counter response is flat over approximately 200 volts the combined counter and electronic system is highly stable. Over the past few years our principal difficulties have been electronic component and power line failures.

(f) Temperature Coefficient of Pile and Detection System

The change of neutron counting rate as a function of room temperature was studied at Climax over a period of time sufficient for the electronic apparatus to attain temperature equilibrium with the room. A temperature range of 20°C was obtained for this measurement, and a least squares calculation gives a local temperature coefficient $T(\text{local}) = 0.00 \pm 0.04$ percent/°C. The pile interior did not vary more than 5° because of its large heat capacity, hence the average temperature of the thermal neutrons within the pile remained essentially constant.

A detailed search was made for a possible influence of the local diurnal temperature upon the neutron counting rate. Piles D-1 and D-3 were enclosed in the same laboratory at Climax. A Ra-Be neutron source was placed in Pile D-1, and the counting rate was corrected for pressure variations. Simultaneously the pressure corrected counting rate from D-3 was studied during one of the periods when there was a recurring 24-hour cycle of intensity larger than the mean of the kind we have found to exist in the low energy component.[8] The results are shown in Fig. 12. Clearly the large daily cycle is not produced by local temperature effects. These results are in agreement with our earlier evidence of a negligible local temperature coefficient.

Since the temperature coefficients of all pressure indicators are -0.04 mm Hg/°C or less the instrumental temperature effects are negligible.

(g) Pressure Indicator Response

Two types of atmospheric pressure indicators have been compared to determine the precision with which a pressure indicator follows pressure changes as a function of time, i.e., dP/dt. For large values of dP/dt around a mean pressure of ~ 500 mm Hg a recording Microbarograph (Friez) displayed a time lag up to 0.5 hr in recording true pressure when compared with a highly corrected aneroid type dial pressure indicator (Wallace-Tiernan Company). The maximum error introduced in the recording instrument during large dP/dt was 1 mm Hg. This error becomes important for studies of neutron intensity variations whenever time intervals the order of one hour or less are used. Hence, for studies of recurring daily cycles of neutron intensity maxima, an instrument with the response of the aneroid gauge is essential.

VII. THE GEOGRAPHIC DISTRIBUTION OF PILES FOR THE STUDY OF ENERGY DEPENDENCE OF INTENSITY VARIATIONS

Referring to Fig. 7, which gives the specific yields of neutrons from primary protons and per nucleon from alpha-particles, we note that above $\lambda \approx 54°$ at *mountain altitudes* and lower the contribution of low energy particles to neutron production is negligible. Hence, positions on the earth for measuring energy dependence of primary intensity variations were selected between $\lambda = 0°$ and 50°. Compromises were made on the choice of high altitude locations for our laboratories in order to secure adequate ac power facilities, local technical help, and easy access from Chicago. It was important

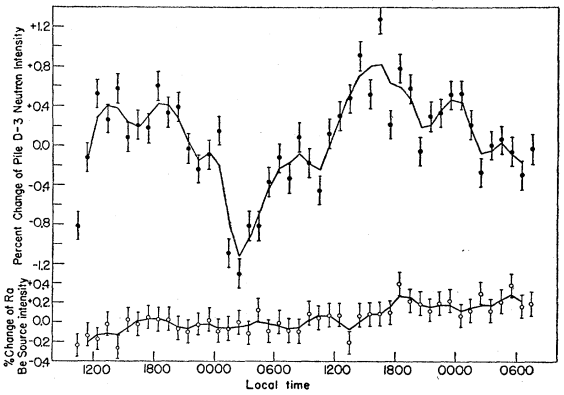

FIG. 12. The upper curve represents the percent changes of neutron production from the nucleonic component as measured by the 12 counter pile, D-3. These data were obtained during an interval when the 24-hour variation or *recurring daily variation* was large. (See reference 8.) The lower curve represents the simultaneous percent changes in pile D-1 where over 94 percent of the neutrons are produced by a Ra-Be source within the pile (see Sec. VIf). The local temperature change during the measurements is $\Delta T = 20$°C.

TABLE II. Continuous operating pile locations on the earth established to determine nucleonic component intensity variations as a function of time and cut-off primary particle momenta.

Name of station and designation	Geomagnetic latitude, λ	Geographic longitude	Mean pressure P and mean atmospheric depth $\bar{X}$ for normalization	Detector design	Film or tape record	Electronic computer log plot	Typical counting rate counts/min	Maximum precision of pressure readings mm Hg at 0°C	Date of *termination* of station or airborne operation
Chicago, Illinois			$P=750$ mm Hg						
C-1	52.6°	87.8°	at 0°C	Paraffin pile	x				Aug., 1950
C-2	N	W		Paraffin pile	x	x	20		Dec., 1950
E-1			$\bar{X}=1018$ g-cm^{-2}	Standard pile	x	x	43	±0.1	
(E-3a)(E-3b)				12 counter lead+ paraffin pile dual electronics	x	x	420		
Climax, Colorado	48°	106°							Oct., 1951
D	N	W	$P=495$	Paraffin pile	x	x	170	±0.1	Sept., 1952
D-1			$\bar{X}=672$	Standard lead	x		680		
D-3				12 counter pile lead+ paraffin	x	x	7000	±0.025	Sept., 1952
(D-3a)(D-3b)				6+6 counter pile. Dual electronics	x	x	7000		
Sacramento Peak, New Mexico F-1	42° N	106° W	$P=545$ $\bar{X}=740$	Standard pile	x	x	368	±0.1	
Mexico City, Mexico M-1	29° N	99° W	$P=584$ $\bar{X}=792$	Standard pile	x	x	160	±0.1	Oct., 1951
M-1a				Same; under absorber	x	x	100		
Huancayo, Peru H-1	0.5° S	75° W	$P=512$ $\bar{X}=694$	4-counter lead+ paraffin pile	x	x	380	±0.1	
Airborne piles, B-29 aircraft	0° to 65°		—	See reference 24 Geometry A Geometry B, C	x		—	See reference 4	July, 1948 to Nov., 1949
RF-80 jet type aircraft	40° to 69°		—	Lead+ paraffin pile *or* Fast neutron detector	x		—	See reference 4	Sept., 1950 to Dec., 1952

to select stations with widely dissimilar meteorological conditions so that the effect of temperature variations could be estimated.

In Table II we have indicated the distribution of our monitoring piles from 1948 through the present.

It is clear from earlier studies of time variations[4] at high altitudes that crucial evidence regarding the nature of intensity variations can be obtained in aircraft flying over a wide latitude range at constant atmospheric depth. Following the studies with the B-29 craft we decided to design subminiature automatic detection equipment which could be installed in the nose section of type RF-80 jet aircraft. Among the detectors is a pile geometry for studying both time variations and local neutron production in elements.

The jet aircraft has proved capable of covering within the order of a day a geomagnetic latitude range of $\sim 40°$–$63°$ at atmospheric depths as low as $x \approx 200$ g-cm^{-2}. This is precisely the region which is inaccessible for mountain observation. The precision of airborne pressure and navigation measurements has been discussed.[4]

VIII. SECONDARY RADIATION INTENSITY VARIATIONS OF METEOROLOGICAL ORIGIN

In this section we shall discuss the effect of atmospheric pressure and temperature upon the observed pile neutron intensity. These effects constitute interference effects in studying the true primary intensity variations.

TABLE III. Parameters for partial correlation studies of atmospheric pressure variations and nucleonic component intensity.

Parameters N	Units days	1st period 1951 7–14 to 8–19 29	2nd period 1951 8–20 to 9–19 24	3rd period 1951 9–20 to 10–17 24
a_{IP}	%/mm Hg	−1.36	−1.12	−1.18
R_P		5.7	4.5	8.4
r_{PQ}		−0.39	−0.22	−0.25
$a_{IP,Q}$	%/mm Hg	−0.88	−0.87	−1.03
$R_{P,Q}$		6.3	7.2	12.1

(a) Atmospheric Pressure Changes—The Mass Effect

The local neutron production rate in a pile at geomagnetic latitude λ and atmospheric depth x is a function of the mass of air x above the pile. Although the pile is an omni-directional detector, the incident nucleonic component is peaked around the vertical direction for large x and, therefore, a measurement of the local atmospheric pressure is a measure of the average air mass over the detector. It is clear from the fact that the absorption mean free path of the star producing radiation is the order of 150 g-cm^{-2} that changes of air mass produce changes in the nucleon flux entering the pile. We consider in this section the determination of the pressure coefficient α of the low energy nucleonic component as a function of λ and its relationship to the absorption mean free path $L(\lambda, x)$ for atmospheric star and neutron production.

There are difficulties in determining the pressure coefficient α of the nucleonic component at a fixed position x, λ. First, as we have already shown, large intensity variations of the order of 5 percent occur within the atmosphere owing to primary intensity variations in periods of time significantly shorter than one month. Therefore, unless the pressure variations are very large in a corresponding interval of time, an accidental correlation between trends in primary intensity changes and local pressure may be observed. Second, there are seasonal trends in pressure and irregular cosmic-ray intensity changes. These effects yield a spurious barometric coefficient.

To illustrate, let us compute the precision with which α may be determined by a statistical study of the uncorrected neutron intensity data. Let δA_i be the departure of any physical quantity A_i from its mean value $\bar{A}$. Let I_i be the daily average of neutron intensity I on day i, P_i the daily average of the station pressure, and assume a regression of I on P:

$$\delta I_i = a_{IP}\delta P_i.$$

The zero-order regression coefficient a_{IP} is given by $(a_{IP} \equiv \alpha)$

$$a_{IP} = r_{IP}\sigma_I/\sigma_P,$$

where σ_I, σ_P, and r_{IP} are the standard deviations and correlation coefficient of δI, δP during the N day period under study. The ratio of a_{IP} to its standard deviation is

$$R_P = N^{\frac{1}{2}}|a_{IP}|\sigma_P/\sigma_{I,P},$$

where $|a_{IP}|\sigma_P$ is the standard deviation of the variation $a_{IP}\delta P$ in I explained by the pressure dependence and $\sigma_{I,P}$ is the standard deviation of the residual variation $(\delta I - a_{IP}\delta P)$ not explained by the pressure dependence.

For periods of the order of one month and for neutron piles located at large x and $\lambda = 40$ to 50°,

$$\sqrt{N} \simeq 5, \qquad |a_{IP}| \approx 1.0 \text{ percent/mm Hg},$$
$$\sigma_P \approx 2.5 \text{ mm Hg}, \qquad \sigma_{I,P} \approx 2.0 \text{ percent},$$

where the percents are computed from the mean neutron intensity. Thus, $R \approx 6$, and the pressure coefficient is determined with a standard deviation of ≈ 17 percent. Clearly, this method leads to a wide spread in the computed values for α based upon the uncorrected neutron intensity data.

Since the residual variation $\sigma_{I,P}$ has been ascribed to world-wide temporal variations of the primary radiations (and it is shown in part (c) below that temperature variations are not comparable in magnitude to pressure variations), the regression equation may be improved by including an additional variable δQ_i to take into account the primary intensity variation. Hence,

$$\delta I_i = a_{IP,Q}\delta P_i + a_{IQ,P}\delta Q_i.$$

The first-order regression coefficient $a_{IP,Q}$ is given by

$$a_{IP,Q} = \frac{[r_{IP} - r_{IQ}r_{PQ}]}{[1 - r_{PQ}^2]} \times \frac{\sigma_I}{\sigma_P}.$$

$a_{IP,Q}$ differs from a_{IP} if $r_{PQ} \neq 0$. The ratio of $a_{IP,Q}$ to its standard deviation is

$$R_{P,Q} = (1 - r_{PQ}^2)^{\frac{1}{2}} N^{\frac{1}{2}} \frac{|a_{IP,Q}|\sigma_P}{\sigma_{I,PQ}}.$$

$\sigma_{I,PQ}$ is the standard deviation of the residual variation $(\delta I - a_{IP,Q}\delta P - a_{IQ,P}\delta Q)$ unexplained by the regression variables.

The daily averages of the primary intensity are not measured directly, but since this is a world-wide effect extending to high primary energies,[30] we may substitute for Q the corrected daily averages measured by another (far removed) cosmic-ray station at approximately the same latitude. Data satisfactory for this purpose have been obtained from the published[31] ionization chamber measurements of Sittkus at Freiburg, Germany (5500 miles from Climax). His data are corrected for both pressure and temperature variations and hence represent variations of primary intensity. When the above methods are applied to the Climax pile (D-1) data

[30] W. Fonger, thesis, University of Chicago, unpublished.

[31] A. Sittkus, *Sonnen-Zirkular* (Fraunhofer Institute, Freiburg-in-Baden, 1951), p. 4. Hourly intensity averages are published quarterly.

during a three months period, July–October, 1951, parameters for the regression equation and the regression coefficient have been tabulated in Table III. By introducing the Q variable from the Freiburg data, the statistical error on the barometric coefficient has been markedly reduced ($R_{PQ}>R_P$) and a spurious value for the barometric coefficient has been avoided.

The best value obtained from this analysis is a $a_{IP,Q}\equiv\alpha=(-0.96\pm0.06)$ percent/mm Hg, and since $L=(10/\alpha)13.56$ g-cm^{-2}, this corresponds to an absorption mean free path $L=142\pm9$ g-cm^{-2}. The negative sign for α indicates an inverse relationship between observed change of neutron intensity and atmospheric pressure. We do not find that α for pure paraffin piles is significantly different from paraffin and lead piles. The results appear to be in agreement with the sea level determinations of α already published.[7,22]

(b) The Latitude Dependence of the Pressure Coefficient

An independent determination of the barometric coefficient for local neutron production is obtained by measuring the absorption mean free path of the radiation incident on a pile. Measurements have already been reported[24,25] for $L(\lambda, x)$ in the range $x=200$–600 g-cm^{-2} and $\lambda=0°$–$65°$ using elementary pile structures transported in B-29 type aircraft. The values for L increase from 150 g-cm^{-2} at $\lambda=54°$ to 210 g-cm^{-2} at $\lambda=0°$ in agreement with production of neutrons in the free atmosphere.[4] Recently, these local production measurements have been extended to large atmospheric depths at 40° and 52°.[13] Briefly, the results clearly show that the average nucleon energy in the nucleon chain degenerates to such an extent that, for example, at 40° where $L\approx175$ g-cm^{-2} at $x\lesssim500$ g-cm^{-2} the mean free path changes to $L_{40°}=145\pm3$ g-cm^{-2} for $x\gtrsim700$ g-cm^{-2}. At atmospheric depths $x>700$ g-cm^{-2} the value for L becomes practically *independent* of λ using a paraffin and lead pile. This has been verified by the following measurements at $\lambda=0°$ in Peru using a standard 2-counter paraffin-lead pile. The local neutron production was measured with and without lead at atmospheric depths $\bar{x}=611$ g-cm^{-2} (Cercapuquio) and at $\bar{x}=694$ g-cm^{-2} (Huancayo). These two precise points yield the value $L=149\pm9$ g-cm^{-2} with and without lead.

We thus conclude that the family of absorption curves in reference 4 *bend downward* at large atmospheric depths to approach a mean free path independent of primary particle momentum, namely $L=145$ g-cm^{-2}. This corresponds to a nucleonic component pressure coefficient $\alpha=-(0.94\pm0.03)$ percent/mm Hg.

We use this value of α to correct neutron intensity data for pressure changes at the pile locations given in Table II. Each pile is assigned a mean atmospheric depth $\bar{x}$, and the observed counting rate is corrected for pressure variations to give the counting rate at $\bar{x}$.

The conditions under which a pure carbon or paraffin pile has a significantly different α from a paraffin plus lead pile appear to be restricted to small atmospheric depths at high latitudes. This behavior is described elsewhere and is not related to reported differences of α for carbon or paraffin plus lead piles near sea level.[7,22]

(c) Atmospheric Temperature or Density Effects

For a detector of secondary particles located at λ, x within the atmosphere the measured intensity may be a function of the atmospheric temperature distribution above the detector. Changes of atmospheric temperature produce changes in air density or changes in the height of a given pressure region above a fixed detector position. Since π- and μ-mesons are among the principal secondary particles, it is clear that, owing to their relatively short mean lives, any changes of air density will change the ratio of decay to nuclear capture rates for π-mesons and will change the time of flight required for μ-mesons to reach the detector. As a result changes of meson intensity are produced in meson sensitive detectors. This problem has been studied using ion chambers and counter telescopes. In this section we shall discuss the atmospheric temperature problem with respect to nucleonic component intensity or, more specifically, to local neutron production in piles.

If the entire neutron local production in a pile were related to the primary radiations only by secondary nucleons, there would be no observable temperature effect for the nucleonic component since nucleons have long mean lives. However, we must consider the real physical situation where secondary mesons are also produced which, in turn, may lead either to further high energy nucleon production in the atmosphere or

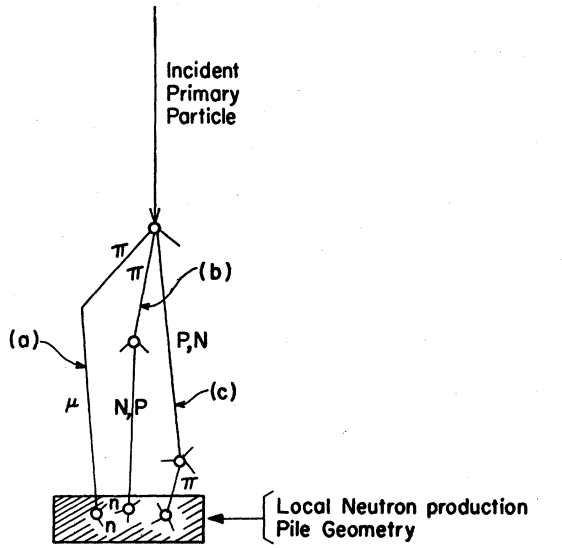

FIG. 13. Atmospheric temperature sensitive links in the nucleonic cascades or chains. Compare this diagram with Fig. 3 for symbols. The magnitude of the temperature coefficient for the nucleonic component is discussed in Sec. VIIIc.

star production within the pile. We define these processes in the nucleonic component as *meson links* in the nucleonic component; typical examples of meson links within a nucleon cascade or chain are shown in Fig. 13.

We consider first the contribution of nuclear disintegrations locally produced by μ-mesons [Fig. 13(a)]. There are two cases; first, high energy μ-meson star production and, second, slow μ-meson capture. It is well established that high energy μ-mesons produce nuclear disintegrations yielding neutrons.[32,33] The contribution of neutrons produced by high energy μ-mesons is <2 percent of the total local neutron rate in lead at sea level.[26] This is in agreement with the observed μ-meson cross section for nuclear interactions, $\sigma_\mu=1\times10^{-29}$ cm^2/nucleon. These values are consistent with the upper limits for local neutron production by μ-mesons at high altitudes. Since L_μ/L_{nucleon} is very large the sea level pile (see Table II) has the largest contribution of neutrons from μ-mesons and, therefore, represents an upper limit for this effect. Thus, <2 percent of the pile neutron production is a function of the μ-meson temperature coefficient, T_μ. The magnitude of T_μ has been determined for both ion chamber and counter telescope as $T_\mu=-0.18$ percent/°C.[34] Since for adequate lead shielding the response of these detectors is practically 100 percent from μ-mesons, we shall use this as the upper limit for the corresponding temperature coefficient $T_\mu{}^N$ in the neutron pile. Hence, $T_\mu{}^N\approx-0.02T_\mu\approx-0.004$ percent/°C, where the temperature changes occur in the 200–1000 mb pressure range of the atmosphere.

Since the positive temperature coefficient[35] T_π, associated with telescope and ion chamber μ-meson measurements is $T_{\pi,\mu}=+0.12$ percent/°C, it is clear that the upper limit for the positive effect for piles is $\lesssim+0.002$ percent/°C, where the temperature changes occur in the 50–150-mb pressure level.

The second case we consider is negative μ-meson capture within the pile ($\mu^-+P\rightarrow N+\nu$). The relative contribution of this process to the total local neutron production is greatest for the sea level pile at Chicago and decreases with altitude. The average neutron multiplicity for this process is approximately $\bar{\nu}_\mu=2$. If we compute the number of μ^- mesons which stop in the lead and assume as an upper limit that each stopped μ^- produces two neutrons, then the neutron production rate from this source is <3 percent of the total local production within the Chicago pile. Thus the temperature coefficient for this process is estimated as $T_\mu{}^N<-0.03(0.18)$ percent/°C$=0.005$ percent/°C at sea level.

The latitude effect for local neutron production at sea level is approximately a factor of 2 between 0° and 54°, hence, the value of $T_\mu{}^N$ and $T_{\pi,\mu}{}^N$ will increase only by a factor of 2 for equatorial sea level observations. Now, since we are concerned with atmospheric temperature changes generally *less* than $\Delta T\approx30$°C, the total atmospheric temperature correction for μ-meson links in the nucleonic component is negligible.

The problem of estimating the π-meson link [Fig. 13(b)] temperature coefficient $T_\pi{}^N$ is more difficult owing to the lack of extensive direct experimental evidence of the behavior of π-mesons in the atmosphere. We examine first the case where a high energy π-meson undergoes nuclear capture in the atmosphere to produce a nucleon capable of entering the pile to contribute to local star production. We know that the π-meson mean life is $\tau_\pi=2.5\times10^{-8}$ sec, and we assume both (1) that the cross section for nuclear capture is geometrical and (2) that the intensity-energy distribution of π-mesons has the form given by Camerini *et al.*[36] If the proper mean life of a π-meson is τ_π and the apparent mean life is $\tau_\pi{}^*$ then $\tau_\pi{}^*=\tau_\pi/(1-\beta^2)^{\frac{1}{2}}$ and the observed mean range R^* in centimeters is $R^*=(\tau_\pi/m_\pi)p$, where m_π and p are the π-meson rest mass and momentum, respectively. Thus, if L is the π-meson mean free path in g-cm^{-2} then the probability for π-meson capture is $(R^*/L)\rho$, where ρ is the density of air. Hence,

$$T^1=\frac{d}{dT}\left(\frac{R^*}{L}\rho\right)=+\frac{R^*}{L}\frac{d\rho}{dT}$$

for π-mesons of momentum p. The expression for T^1 must be integrated over the entire π-meson momentum spectrum at the atmospheric density ρ to obtain the π-meson temperature coefficient $T_\pi{}^N$. This is an upper limit since only a small fraction of the captured π-mesons will produce nucleons which may reach the detector. The probability of π-meson capture becomes appreciable above $\sim$30–50 Bev. The number of particles above this energy limit is $\ll0.01$ of the total number throughout the energy spectrum, and, if we assume that the T_π measured by a meson telescope is $+0.12$ percent/°C arising from the fraction which decay, then $T_\pi{}^N<-0.01T_\pi=-0.001$ percent/°C. This appears to be a negligible coefficient for local neutron production from high energy π-meson links at small atmospheric depths.

At lower π-meson energies the contribution of meson links of the kind shown in Fig. 13(b) is difficult to determine. However, the upper limit of this component of the temperature effect undoubtedly becomes vanishingly small due to the rapidly increasing probability for π-meson decay with decreasing energy.

The second π-meson link case we consider is the nearby creation of low energy π-mesons which enter the pile to produce nuclear disintegrations, Fig. 13(c). Measurements in photographic emulsions of the ratio

[32] G. Cocconi and V. Cocconi Tongiorgi, Phys. Rev. **84**, 29 (1951).
[33] A. M. Conforto and R. D. Sard, Phys. Rev. **86**, 465 (1952).
[34] A. H. Compton and R. N. Turner, Phys. Rev. **52**, 799 (1937); D. W. N. Dolbear and H. Elliot, J. Atmos. Terr. Phys. **1**, 215 (1951).
[35] A. Duperier, Proc. Phys. Soc. (London) **A62**, 684 (1949).
[36] Camerini, Fowler, Lock, and Muirhead, Phil. Mag. **41**, 415 (1950).

(nucleon produced star)/(π-meson produced star) gives an upper limit of 5 percent for π-star production and, hence, neutron production by π-mesons.[37] If we assume that the low energy π-meson temperature coefficient is as large as T_π then the maximum contribution to $T_\pi{}^N$ from the low energy mesons is $T_\pi{}^N(\text{low})<0.05T_\pi$ $=-0.006$ percent/°C *local* temperature at $\lambda=50°$. Since π-meson production has approximately the same altitude dependence as the nucleonic component $T_\pi{}^N(\text{low})$ is principally dependent on λ. At $\lambda=0°$ we estimate an upper limit of $T_\pi{}^N(\text{low})<-0.02$ percent/°C. A direct test for this effect was discussed in Sec. VI where it was shown that surface and room temperature changes do not produce a measurable local temperature dependence.

In summary, the estimated *upper* limit of $T_\pi{}^N$ for all π-meson links is ~-0.02 percent/°C or less under the most unfavorable conditions for pile operation. This value is an order of magnitude smaller than T_π for counter telescopes or ion chambers.

We have neglected contributions from heavy mesons[38] of mass $>m_\pi$ due to their extremely short mean lives and small rate of production. The short mean life of π^0 precludes the observation of any temperature dependent γ-n production within the pile. Although atmospheric showers produce neutrons and have a large temperature coefficient, their frequency is entirely too low to contribute to the pile temperature coefficient. We conclude from the above discussion that the *total* temperature coefficient of the nucleonic component, namely $T^N=[T_\mu{}^N+T_\mu{}^{-N}+T_\pi{}^N+T_\pi{}^N(\text{low})]<-0.02$ percent/°C at $\lambda=0°$; $T^N<-0.006$ percent/°C at $\lambda=50°$. Clearly, the experimental errors in correcting for pressure variations are much larger than T^N. We henceforth treat the temperature coefficient as negligible unless explicitly stated otherwise.

The determination of T^N by correlation analysis using radiosonde temperature *vs* pressure data is fraught with difficulties of the type discussed in Sec. VIIIa in the pressure coefficient studies, e.g., accidental correlations of temperature with primary intensity variations. By the use of the method described in Sec. VIIIa which takes into account the primary intensity variations, the partial correlation coefficient was determined with the Chicago pile for the mean temperature variations in the pressure interval 200–850 millibars at Chicago. Two months of data were studied. For the first month $T^N=+0.10\pm0.12$ percent/°C; for the second month $T^N=+0.02\pm0.15$ percent/°C. The detailed discussion in the earlier portion of this section shows that any meson temperature coefficient for the nucleonic component will be negative. Hence, we conclude from the study of the two months of data that the measured temperature coefficient $T^N\approx0.0$. These correlation studies are being continued.

(d) Additional Local Weather Effects

Since the absorption mean free path is 145 g-cm^{-2} for the nucleonic component incident on a pile a large snow or ice deposit on the roof protecting the apparatus will change the observed pile neutron intensity. For example, a 30-cm snow deposit over the pile is equivalent to ~3 g-cm^{-2} H_2O; this is equivalent to a pressure change of 2.2-mm Hg which in turn would produce a decrease in neutron counting rate of 2.1 percent. Therefore, either the observed counting rate must be corrected for this effect or the data should be discarded for periods when snow deposits lie over the equipment. The piles located at Climax, Colorado where this effect is serious, have now been mounted in a metal housing above the snow level with a heated metal roof designed to melt the snow as it falls during the winter months. The snow deposit problem elsewhere (see Table II) is not serious.

Rainfall changes the local production rate and moderation of neutrons in the atmosphere. These effects would be observed by a bare BF_3 counter, but as pointed out in Secs. V and VI the use of a local neutron producing pile eliminates the rain effect.

Natural radioactivity or fission-product activity in the vicinity of a detector may change by more than an order of magnitude as a result of concentration by rainfall or winds. This change in "background ionization" within a detector is serious for an unshielded ion chamber but has no effect on a BF_3 proportional counter.

SUMMARY

We have demonstrated how the continuous observation of variations of the primary radiations may be extended to lower energies than has been possible using charged particle detectors. Further, we are able to relate the variations of local neutron production in pile geometries located within the atmosphere to variations in the primary radiation. Consequently, the *energy* dependence of the low energy time variant portion of primary radiation intensity may be studied.

We examined the meteorological effects which may interfere with these measurements, e.g., pressure and temperature. The pressure coefficient is large and essentially independent of geomagnetic latitude for atmospheric depths $x\gtrsim600$ g-cm^{-2}. The upper limit of the temperature coefficient of the nucleonic component has been computed from reasonable assumptions regarding the behavior of π- and μ-mesons in the atmosphere and their contributions to the nucleonic component, yielding an upper limit of ~0.1, the magnitude of the temperature coefficient for charged particle detectors. It is notable that this coefficient for the pile is negative and appears to be negligibly small.

[37] Bernardini, Cortini, and Manfredini, Phys. Rev. **76**, 1792 (1949).

[38] For charged particle detectors the effect of K-mesons is discussed by L. Verlet, Phys. Rev. **86**, 792 (1952).

Some preliminary reports of the results we have obtained from the system of piles described in this paper have already been published. For example, series of 27-day primary intensity peaks have been found[9] with an average amplitude of ~ 5 percent, and it has been shown that this variation extends to primary energies > 10 Bev for protons.[39] These intensity changes and their appearance with small amplitude even at high primary energies have been recently confirmed by Neher and Forbush[40] and Fonger.[30]

We conclude that after correcting all pile intensity data for atmospheric pressure variations the influence of the atmosphere upon intensity variations is negligible for our present studies. However, from the discussion in Sec. II it is clear that we have yet to demonstrate to what extent, if any, variations of geomagnetic or geoelectric fields may interfere with observations of primary intensity variations. In forthcoming papers we shall describe experiments which bear on this question.

It has been possible to establish the pile locations given in Table II only through the cooperation of several groups. Dr. W. O. Roberts of the High Altitude Observatory has provided enthusiastic assistance in making available the Climax location for continuous monitoring. The U. S. Air Force has generously provided facilities at Sacramento Peak. G. Schnable, R. Allen, R. Cook, and R. Hansen have maintained these two locations even under the most severe conditions. Professor M. S. Vallarta and the University of Mexico have graciously provided facilities for the apparatus in Mexico City, and Dr. Merino Coronado has supervised the operation of this pile. In Huancayo, Peru, Mr. Albert Giesecke, Jr., and the Instituto Geofisico de Huancayo have kindly provided facilities for continuous operation under Mr. H. Goller. In Chicago, Mr. J. Firor and Mr. W. Dumke have aided in design and operation problems.

[39] Simpson, Fonger, and Wilcox, Phys. Rev. **87**, 240 (1952).
[40] H. V. Neher and S. E. Forbush, Phys. Rev. **87**, 889 (1952).